

Quantum entanglement transfer assisted via Duffing nonlinearity

D. R. Kenigoule Massembele,^{1,*} P. Djorwé,^{1,2,†} Amarendra K. Sarma,^{3,‡} and S. G. Nana Engo^{4,§}

¹*Department of Physics, Faculty of Science, University of Ngaoundere, P.O. Box 454, Ngaoundere, Cameroon*

²*Stellenbosch Institute for Advanced Study (STIAS), Wallenberg Research Centre at Stellenbosch University, Stellenbosch 7600, South Africa*

³*Department of Physics, Indian Institute of Technology Guwahati, Guwahati 781039, India*

⁴*Department of Physics, Faculty of Science, University of Yaounde I, P.O. Box 812, Yaounde, Cameroon*

We propose a scheme to enhance quantum entanglement in optomechanical system that is based on Duffing nonlinearity. Our benchmark system consists of an electromagnetic field that is driving two mechanically coupled mechanical resonators. One of the mechanical resonators support a Duffing nonlinear term, while the other is free of it. The phonon hopping rate is θ -phase-dependent that induces a synthetic magnetism, which triggers Exceptional Points (EPs) singularities in the system. Without the Duffing nonlinear term, the entanglement between the electromagnetic field and the mechanical resonators is generated. This entanglement features the sudden death and revival phenomenon, where the peaks happen at the multiple of $\theta = \frac{\pi}{2}$. As the Duffing nonlinearity is accounted, the bipartite entanglement involving the nonlinear resonator vanishes. However, there is an entanglement transfer from the resonator supporting the nonlinear term towards the one that is mechanically coupled to it. This nonlinearly induced entanglement is robust against thermal fluctuation, and more stable compared to what is generated without the nonlinear term. This work paves a way to a generation of quantum entanglement using nonlinear resources, enabling quantum technology such as quantum information processing, quantum sensing, and quantum computing in complex systems.

Keywords: Optomechanics, entanglement, exceptional point, Duffing nonlinearity, synthetic magnetism

I. INTRODUCTION

Optomechanics is a research field that deals with the interactions between electromagnetic field and mechanical motion. Recently, this field became an interesting platform to investigate plethora of physical phenomena both in classical [1–5] and quantum regime [6–9]. In the classical domain, numerous phenomena including synchronization [10–13], nonlinear dynamics [14–17], and chaos-like behaviors [18, 19] have been reported. In the quantum regime, interesting properties of quantum correlations [20–22] and nonclassical states [23–25] were revealed. Such quantum effects constitute a hallmarks of quantum physics, particularly the squeezed [26] and entangled states [27–29]. Indeed, quantum entanglement is a prerequisite for quantum technology, such as quantum information processing [30, 31], quantum computing [32], and sensing [33].

Owing to the important role played by entanglement in number of quantum technology, there is an urgent quest to come up with new mechanisms to generate entangled states which are robust enough against decoherence and thermal fluctuation. For this purpose, some nonlinearities such as cross-Kerr effect and parametric amplifier have been used to enhance quantum entanglement in optomechanics for instance. Exceptional Points (EPs), which are Non-Hermitian degeneracies, have been also recently used as a tool to engineer stable and robust entanglement [34]. Despite the fact that EPs improve the generation of entanglement, it is therefore not an easy task to synthesize them in a given physical system.

In fact, the system parameters most fulfill some requirements such as balanced gain-loss for instance, which is usually not a trivial condition to meet. Recently, this requirement has been relaxed through the synthetic magnetism, which allows the engineering of EPs in a lossy system. This approach has led to a generation of noise-tolerant optomechanical entanglement via a dark-mode breaking [35].

The aim of the current work is to combine the effect of nonlinearity together with the synthetic magnetism effect to generate robust quantum entanglement. Our benchmark system consists of an electromagnetic field that is driving two mechanical resonators, which are mechanically coupled through a phase-dependent phonon-hopping. This phase-dependency is reminiscent of the synthetic magnetism, and it triggers EPs singularities in the system. To account for nonlinearity in our proposal, we assume that one of the mechanical resonators supports a Duffing nonlinear term [36]. In our investigation, we pointed out that bipartite entanglement vanishes whenever the resonator supporting this nonlinear is involved. However, there is an entanglement transfer assisted by this Duffing nonlinearity towards the other connected resonator. Moreover, the nonlinear term enhances stability of the system, enabling further entanglement for strong driving strength. Furthermore, the nonlinearly induced entanglement is robust against thermal fluctuation compared to what is generated without the nonlinear term. This work shows how the Duffing nonlinearity can be used to enhance quantum entanglement through a transfer phenomenon. Our proposal sheds light on the exploration of nonlinear effects to generate entanglement, and it constitutes a step towards information processing and quantum computing in complex systems.

The rest of the work is organized as follows. In section II, we describe the model, the related dynamical equations, and presents the linear stability of the system. The entanglement and the effect of the Duffing nonlinearity are carried out in Section III, while the work is concluded in Section IV.

*Electronic address: kenigoule.didier@gmail.com

†Electronic address: djorwepp@gmail.com

‡Electronic address: aksarma@iitg.ac.in

§Electronic address: serge.nana-eng@facsciences-uy1.cm

II. MODEL AND DYNAMICS

Our benchmark system is sketched in Fig.1, where an electromagnetic field (mode a) is driving two mechanical resonators (modes b_j), which are mechanically coupled through a phonon hopping J_m . The phonon hopping term exhibits a synthetic magnetism through the phase modulation θ , and the first resonator supports a Duffing nonlinearity captured by its amplitude η .

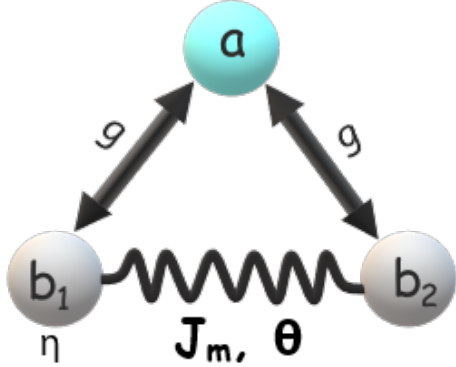


FIG. 1: Sketch of our benchmark optomechanical system. An electromagnetic field (mode a) is driving two mechanically coupled mechanical resonators (b_j). The phonon hopping (J_m) between the two mechanical resonators is modulated through the phase θ that induces a synthetic magnetism. The optomechanical coupling between the electromagnetic field and each mechanical resonator is denoted by g .

In the frame rotating at the driving frequency ω_p , our system is described by the following Hamiltonian ($\hbar = 1$):

$$\begin{aligned}
 H = & -\Delta a^\dagger a + \sum_{j=1,2} \omega_j b_j^\dagger b_j - g a^\dagger (b_j + b_j^\dagger) \\
 & + J_m (e^{i\theta} b_1^\dagger b_2 + e^{-i\theta} b_1 b_2^\dagger) + iE^{in} (a^\dagger + a) \\
 & + \frac{\eta}{2} (b_1 + b_1^\dagger)^4, \quad (1)
 \end{aligned}$$

where $a(a^\dagger)$ and $b_j(b_j^\dagger)$ are respectively the annihilation (creation) bosonic operators of the cavity field and for the j^{th} mechanical resonator (having frequency ω_j). The detuning is defined as $\Delta = \omega_p - \omega_c$, where ω_c is the cavity frequency. The other parameters are the optomechanical coupling g , for each resonator, and the amplitude of the driving field E^{in} . Using the Heisenberg equation, the Quantum Langevin Equations (QLEs) from the Hamiltonian Eq.1 yield,

$$\begin{cases}
 \dot{a} = \left(i \left(\Delta + \sum_{j=1,2} g (b_j^\dagger + b_j) \right) - \frac{\kappa}{2} \right) a \\
 \quad + \sqrt{\kappa} \alpha^{in} + \sqrt{\kappa} a^{in}, \\
 \dot{b}_1 = - \left(\frac{\gamma_1}{2} + i\omega_1 \right) b_1 - iJ_m e^{i\theta} b_2 + i g a^\dagger a \\
 \quad - 2i\eta (b_1 + b_1^\dagger)^3 + \sqrt{\gamma_1} b_1^{in}, \\
 \dot{b}_2 = - \left(\frac{\gamma_2}{2} + i\omega_2 \right) b_2 - iJ_m e^{-i\theta} b_1 + i g a^\dagger a \\
 \quad + \sqrt{\gamma_2} b_2^{in},
 \end{cases} \quad (2)$$

where E^{in} has been substituted by $\sqrt{\kappa} \alpha^{in}$ with α^{in} being related to the input power P^{in} as $\alpha^{in} = \sqrt{\frac{P^{in}}{\hbar \omega_p}}$. The cavity and mechanical dissipations are captured by κ and γ_j , respectively. Moreover, a^{in} and b_j^{in} are the zero mean valued noise operators characterized by their autocorrelations functions,

$$\langle a^{in}(t) a^{in\dagger}(t') \rangle = \delta(t - t'), \quad (3)$$

$$\langle a^{in\dagger}(t) a^{in}(t') \rangle = 0, \quad (4)$$

$$\langle b_j^{in}(t) b_j^{in\dagger}(t') \rangle = (n_{th}^j + 1) \delta(t - t'), \quad (5)$$

$$\langle b_j^{in\dagger}(t) b_j^{in}(t') \rangle = n_{th}^j \delta(t - t'), \quad (6)$$

with $n_{th}^j = \left[\exp\left(\frac{\hbar \omega_j}{k_B T}\right) - 1 \right]^{-1}$ represents the number of phonons at temperature T and k_B the Boltzmann constant. To derive the quadratures of our system, the nonlinear set of equations given in Eq.2 can be linearized through the standard linearization process. Indeed operators are splitted over their mean values and fluctuations, $\mathcal{O} = \langle \mathcal{O} \rangle + \delta \mathcal{O}$, where $\mathcal{O} \equiv (a, b_j)$. By setting $\alpha = \langle a \rangle$, and $\beta_j = \langle b_j \rangle$, the dynamical mean values of our system yields,

$$\begin{cases}
 \dot{\alpha} = (i\tilde{\Delta} - \frac{\kappa}{2}) \alpha + \sqrt{\kappa} \alpha^{in}, \\
 \dot{\beta}_1 = - \left(\frac{\gamma_1}{2} + i\omega_1 \right) \beta_1 - iJ_m e^{i\theta} \beta_2 + i g |\alpha|^2 \\
 \quad - 2i\eta (\beta_1 + \beta_1^*)^3, \\
 \dot{\beta}_2 = - \left(\frac{\gamma_2}{2} + i\omega_2 \right) \beta_2 - iJ_m e^{-i\theta} \beta_1 + i g |\alpha|^2,
 \end{cases} \quad (7)$$

and the fluctuation dynamics reads,

$$\begin{cases}
 \delta \dot{a} = (i\tilde{\Delta} - \frac{\kappa}{2}) \delta a + i \sum_{j=1,2} G (\delta b_j^\dagger + \delta b_j) \\
 \quad + \sqrt{\kappa} \alpha^{in}, \\
 \delta \dot{b}_1 = - \left(\frac{\gamma_1}{2} + i\omega_1 \right) \delta b_1 - iJ_m e^{i\theta} \delta b_2 + i(G^* \delta a \\
 \quad + G \delta a^\dagger) - i\Lambda (\delta b_1 + \delta b_1^\dagger) + \sqrt{\gamma_1} b_1^{in}, \\
 \delta \dot{b}_2 = - \left(\frac{\gamma_2}{2} + i\omega_2 \right) \delta b_2 - iJ_m e^{-i\theta} \delta b_1 + i(G^* \delta a \\
 \quad + G \delta a^\dagger) + \sqrt{\gamma_2} b_2^{in},
 \end{cases} \quad (8)$$

where both effective detuning and optomechanical coupling are defined as $\tilde{\Delta} = \Delta + 2 \sum_{j=1,2} g \text{Re}(\beta_j)$ and $G = g\alpha$. From now on, we will assume that α is real, meaning that G is real as well. Moreover, $\Lambda = 24\eta (\Re(\beta_1))^2$ captures the nonlinear process. The fluctuation dynamics in Eq.8 can be put in its compact form,

$$\dot{x} = Ax + y, \quad (9)$$

where $x = (\delta a, \delta a^\dagger, \delta b_1, \delta b_1^\dagger, \delta b_2, \delta b_2^\dagger)^T$, and the noise vector $y = (\sqrt{\kappa} \alpha^{in}, \sqrt{\kappa} \alpha^{in\dagger}, \sqrt{\gamma_1} b_1^{in}, \sqrt{\gamma_1} b_1^{in\dagger}, \sqrt{\gamma_2} b_2^{in}, \sqrt{\gamma_2} b_2^{in\dagger})^T$, and the matrix A is given by:

$$A = \begin{pmatrix} A_{11} & A_{12} & A_{13} \\ A_{12}^T & A_{22} & A_{23} \\ A_{13}^T & A_{23}^T & A_{33} \end{pmatrix}, \quad (10)$$

with

$$A_{11} = \begin{pmatrix} i\tilde{\Delta} - \frac{\kappa}{2} & 0 \\ 0 & -i\tilde{\Delta} - \frac{\kappa}{2} \end{pmatrix}, \quad (11)$$

$$A_2 = \begin{pmatrix} -(\frac{\gamma_1}{2} + i(\omega_1 + \Lambda)) & -i\Lambda \\ i\Lambda & -(\frac{\gamma_1}{2} - i(\omega_1 + \Lambda)) \end{pmatrix}, \quad (12)$$

$$A_3 = \begin{pmatrix} -(\frac{\gamma_2}{2} + i\omega_2) & 0 \\ 0 & -(\frac{\gamma_2}{2} - i\omega_2) \end{pmatrix} \quad (13)$$

$$A_{12} = \begin{pmatrix} iG & iG \\ -iG^* & -iG^* \end{pmatrix}, \quad (14)$$

$$A_{13} = \begin{pmatrix} iG & iG \\ -iG^* & -iG^* \end{pmatrix}, \quad (15)$$

and

$$A_{23} = \begin{pmatrix} -iJ_m e^{i\theta} & 0 \\ 0 & iJ_m e^{-i\theta} \end{pmatrix}. \quad (16)$$

The steady-state equation of our system is obtain by assuming that the mean values in Eq.(7) are not time dependent ($\dot{\alpha} = \dot{\beta}_j = 0$). Following the Routh-Hurwitz criterion, and by using the steady-state values in matrix A, we get the stability diagrams shown in Fig.2.

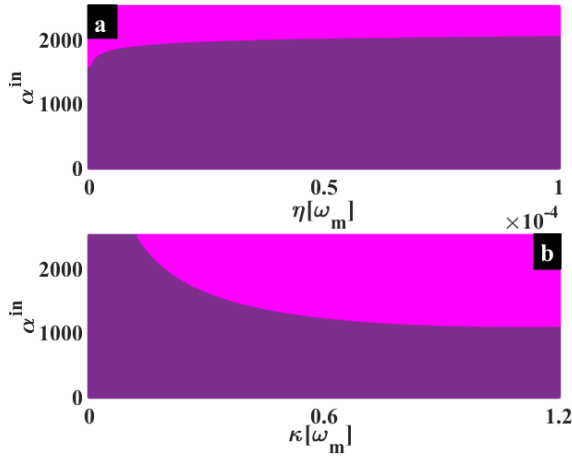


FIG. 2: Stability diagrams. (a) Driving strength α^{in} vs the nonlinear amplitude η for $\kappa = 2 \times 10^{-1}$ and $J_m = 1 \times 10^{-2}$. (b) Driving strength α^{in} vs the cavity decay rate κ for $\eta = 1 \times 10^{-5}$ and $J_m = 1 \times 10^{-2}$. The dark color is stable, while the light color is unstable. The other parameters are $\omega_1 = \omega_2 = \omega_m$, $\gamma_1 = \gamma_2 = 1 \times 10^{-5} \omega_m$, $\Delta = -\omega_m$, $g = 5 \times 10^{-4} \omega_m$ and $\theta = \frac{\pi}{2}$.

Fig.2(a) shows the stability diagram in (η, α^{in}) space, and it can be seen that for a wide range of the Duffing nonlinearity, the system is stable for a driving strength up to $\alpha^{in} \sim 1500 \omega_m^{1/2}$. It can be also seen that as the nonlinearity increases, the stability of the system is slightly improved. For $\eta = 10^{-5} \omega_m$, Fig.2(b) exhibits diagram stability of the system in (κ, α^{in}) space. Similarly as in Fig.2(a), the system is stable for a wide range of κ . These two diagrams are plotted for a synthetic phase of $\theta \sim \pi/2$, and that corresponds to the optimal value of θ around which the logarithmic negativity is strong enough as it will be seen later on.

III. STATIONARY ENTANGLEMENT TRANSFER

To investigate quantum entanglement, we need to define the quadratures and the system must fulfill stability conditions depicted in Fig.2. The quantum quadratures are defined as,

$$\delta x = \frac{\delta a^\dagger + \delta a}{\sqrt{2}}, \delta y = i \frac{\delta a^\dagger - \delta a}{\sqrt{2}}, \delta q_j = \frac{\delta b_j^\dagger + \delta b_j}{\sqrt{2}}, \delta p_j = i \frac{\delta b_j^\dagger - \delta b_j}{\sqrt{2}},$$

with their corresponding noise operators $\delta x^{in} = \frac{\delta a^{in\dagger} + \delta a^{in}}{\sqrt{2}}$, $\delta y^{in} = i \frac{\delta a^{in\dagger} - \delta a^{in}}{\sqrt{2}}$, $\delta q_j^{in} = \frac{\delta b_j^{in\dagger} + \delta b_j^{in}}{\sqrt{2}}$ and $\delta p_j^{in} = i \frac{\delta b_j^{in\dagger} - \delta b_j^{in}}{\sqrt{2}}$.

By using Eq.(8), the system quadratures can be written in its compact form as,

$$\dot{u} = Mu + z, \quad (17)$$

where the quadratures vector is $u^T = (\delta x, \delta y, \delta q_1, \delta p_1, \delta q_2, \delta p_2)$, with the corresponding noise vector set as $z^T = (\sqrt{\kappa} x^{in}, \sqrt{\kappa} y^{in}, \sqrt{\gamma_1} q_1^{in}, \sqrt{\gamma_1} p_1^{in}, \sqrt{\gamma_2} q_2^{in}, \sqrt{\gamma_2} p_2^{in})$, and the drift matrix is:

$$M = \begin{pmatrix} M_1 & M_{12} & M_{13} \\ M_{12}^T & M_2 & M_{23} \\ M_{13}^T & M_{23}^T & M_3 \end{pmatrix}, \quad (18)$$

where the M_i and M_{ij} are blocs of 2×2 matrices defined as,

$$M_1 = \begin{pmatrix} -\frac{\kappa}{2} & -\tilde{\Delta} \\ \tilde{\Delta} & -\frac{\kappa}{2} \end{pmatrix}, \quad (19)$$

$$M_2 = \begin{pmatrix} -\frac{\gamma_1}{2} & \omega_1 \\ -(2\Lambda + \omega_1) & -\frac{\gamma_1}{2} \end{pmatrix}, \quad (20)$$

$$M_3 = \begin{pmatrix} -\frac{\gamma_2}{2} & \omega_2 \\ -\omega_2 & -\frac{\gamma_2}{2} \end{pmatrix}, \quad (21)$$

$$M_{12} = \begin{pmatrix} -2\text{Im}(G) & 0 \\ -2\text{Re}(G) & 0 \end{pmatrix}, \quad (22)$$

$$M_{13} = \begin{pmatrix} -2\text{Im}(G) & 0 \\ -2\text{Re}(G) & 0 \end{pmatrix}, \quad (23)$$

and

$$M_{23} = \begin{pmatrix} J_m \sin \theta & J_m \cos \theta \\ -J_m \cos \theta & J_m \sin \theta \end{pmatrix}. \quad (24)$$

The diagonal blocs matrices M_1 , M_2 and M_3 represent the optical mode, the first and second mechanical mode, respectively. The blocs M_{12} and M_{13} capture the correlations between the driving field with the first and second mechanical resonators, while M_{23} describes the correlations between the mechanical modes. Any bipartite entanglement can be evaluated through the logarithmic negativity by tracing out the

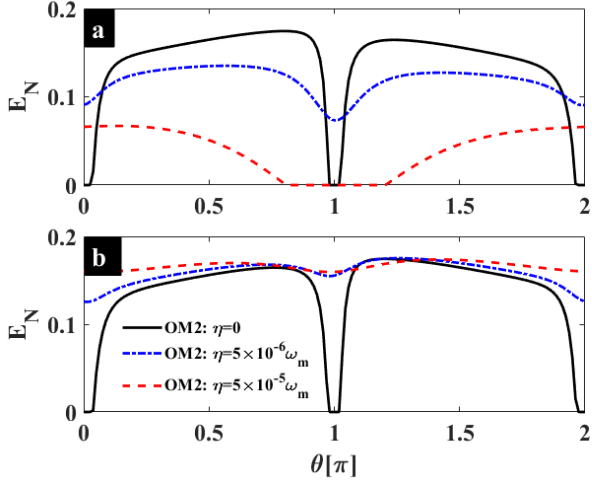


FIG. 3: (a) Entanglement between the electromagnetic field and the nonlinear resonator (mode b_1) versus the synthetic phase θ . (b) Entanglement between the electromagnetic field and the linear resonator (mode b_2) versus the synthetic phase θ . The solid line is without Duffing nonlinearity ($\eta = 0$), while the dash-dotted and dashed lines are for $\eta = 5 \times 10^{-6} \omega_m$ and $\eta = 5 \times 10^{-5} \omega_m$, respectively. We have used $\kappa = 2 \times 10^{-1} \omega_m$, $J_m = 2 \times 10^{-1} \omega_m$, $\alpha^{in} = 1500$ and $n_{th} = 100$. The other parameters are as in Fig.2.

non-necessary third mode. The logarithmic negativity E_N is defined as,

$$E_N = \max[0, -\ln(2\nu^-)], \quad (25)$$

where $\nu^- = \frac{1}{\sqrt{2}} \sqrt{\sum(V) - \sqrt{\sum(V)^2 - 4\det V}}$. V is the covariance matrix with elements defined as,

$$V_{ij} = \frac{\langle (u_i u_j + u_j u_i) \rangle}{2}. \quad (26)$$

When the stability condition is satisfied, the covariance matrix fulfills the following Lyapunov equation,

$$MV + VM^T + D = 0, \quad (27)$$

where $D = \text{Diag}[\frac{\kappa}{2}, \frac{\kappa}{2}, \frac{\gamma_1}{2}(2n_{th} + 1), \frac{\gamma_1}{2}(2n_{th} + 1), \frac{\gamma_2}{2}(2n_{th} + 1), \frac{\gamma_2}{2}(2n_{th} + 1)]$ is the diffusion matrix.

Fig.3 captures the bipartite entanglement between the driving field and the mechanical resonators versus the synthetic phase θ . The interaction with the first mechanical resonator is depicted in Fig.3(a), while entanglement involving the second mechanical resonator is shown in Fig.3(b). In these figures, the solid line represents the case without the Duffing nonlinearity ($\eta = 0$), while the dash-dotted and the dashed lines are for $\eta = 5 \times 10^{-6} \omega_m$ and $\eta = 5 \times 10^{-5} \omega_m$, respectively. For $\eta = 0$, these figures show how the entanglement is modulated over the synthetic phase. Indeed, the entanglement E_N drops around $\theta = n\pi$ for $n \in \mathbb{N}$, and it reaches its optimal value at the vicinity of $\theta = m\pi/2$ where m is an odd number. This dynamical behavior of the entanglement in Fig.3 is reminiscent

of sudden death and revival of entanglement induced through exceptional points in [34]. We would like to underline that the synthetic magnetism phase may also lead to exceptional points in our system for $\theta = m\pi/2$, however, we did not focus our interest on it here. For $\eta \neq 0$, one observes that the overall entanglement becomes weak in Fig.3(a), while it slightly becomes stronger in Fig.3(b). This reveals how the nonlinear term tends to suppress the entanglement on the resonator supporting it, and this entanglement is transferred towards the connected nonlinear-free resonator.

To further highlight this effect of the Duffing nonlinearity, we have plotted Fig.4, where the entanglement is displayed versus the driving strength (Fig.4(a-b)) and over the cavity decay rate (Fig.4(c-d)). In these figures, the solid line is without nonlinearity ($\eta = 0$), and the other lines are for $\eta \neq 0$ as highlighted on the insets. The overall observation is that, the entanglement decreases and seems to switch out on the nonlinear resonator as the nonlinearity is increasing (see Fig.4(a,c)). In the mean time, there is an enhancement of the entanglement on the resonator that is free of the nonlinear term (see Fig.4(b,d)). Beside this sort of entanglement transfer induced by the Duffing nonlinearity, there is also a stability improvement assisted by this nonlinear feature as aforementioned in Fig.2(a). This nonlinear-induced stability triggers more entanglement by extending it over the parameter ranges precluded when the resonators are free of the Duffing term. Therefore, these results shed light on the nonlinear effects which can be used to switch and to enhance entanglement in coupled resonators.

To have a wider view of the Duffing nonlinearity on the entanglement, and to get insight into how this induced entanglement is robust and stable against thermal fluctuation, we refer to Fig.5. The behavior of the entanglement over the Duffing term is depicted in Fig.5(a) for the resonator supporting the nonlinearity, and Fig.5(b) displays the same information of the nonlinear free resonator. The solid line in these figures is for $n_{th} = 0$, and the dashed line is when the thermal phonon number is $n_{th} = 100$. By tracking the solid lines, we can confirm that the nonlinearity enhances the entanglement. As the thermal fluctuation is accounted, the strength of this enhanced entanglement decreases over the nonlinear term. However, the transferred entanglement is robust enough against thermal fluctuation compared to what is generated on the resonator supporting the nonlinearity (compare both lines in Fig.5(a) and Fig.5(b)). The robustness of the transferred entanglement is further highlighted in Figs.5(c,d), where the logarithmic negativity is displayed over the thermal phonon number. By comparing the dashed and dash-dotted lines in these figures, it appears that the transferred entanglement features a better robustness against thermal fluctuation as the nonlinearity is strong enough. This reveals how Duffing nonlinearity can be used as a requirement to foster strong and stable entanglement against thermal fluctuation, leading to an improvement of quantum information processing and quantum computing in complex systems supporting nonlinearities.

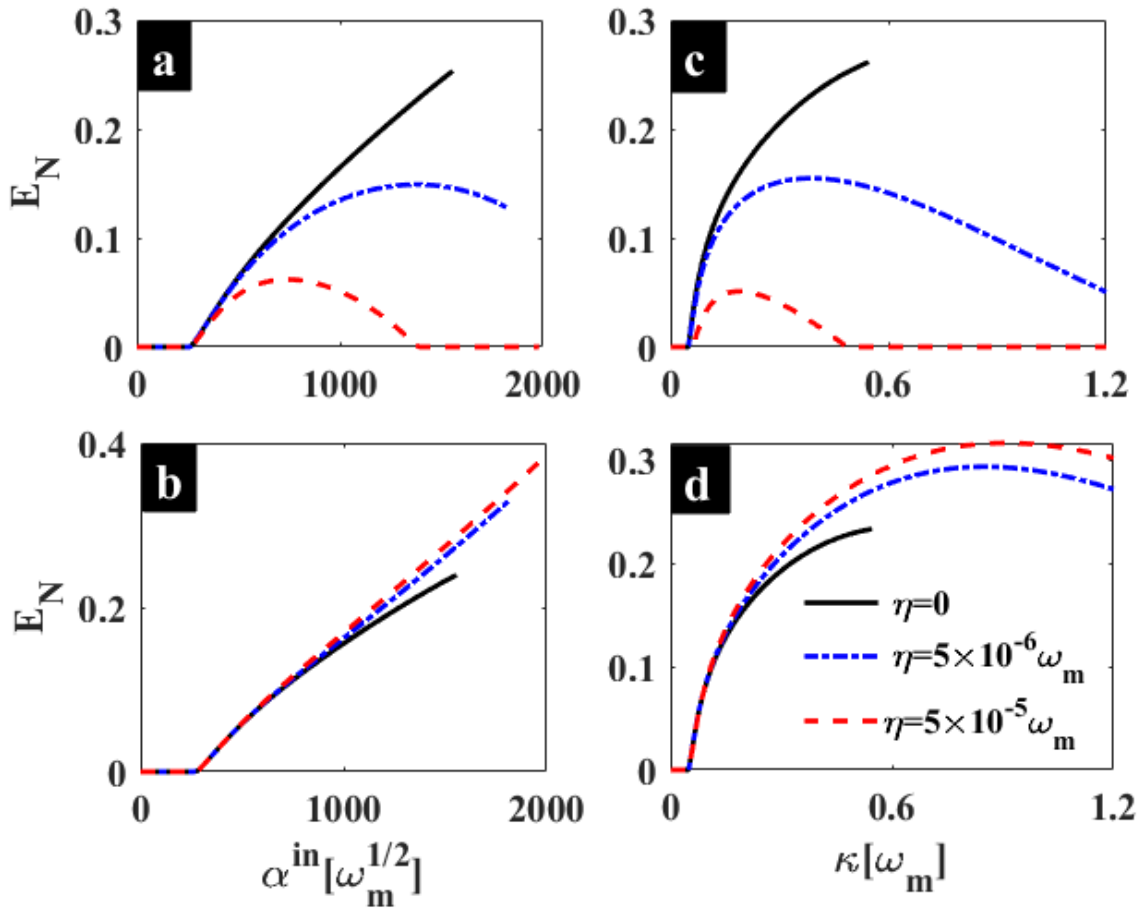


FIG. 4: Entanglement between the electromagnetic field with the nonlinear resonator (a), and with the linear resonator (b) versus the driving field α^{in} . Entanglement between the electromagnetic field with the nonlinear resonator (c), and with the linear resonator (d) versus the cavity decay rate κ . In all these figures, the solid line is without Duffing nonlinearity ($\eta = 0$), while the dash-dotted and dashed lines are for $\eta = 5 \times 10^{-6} \omega_m$ and $\eta = 5 \times 10^{-5} \omega_m$, respectively. The phonon number is $n_{th}^{1,2} = 100$ for all figures, while in (c,d) $\alpha^{in} = 1000$. The rest of the parameters are as in Fig.3.

IV. CONCLUSION

We have investigated stationary entanglement in an optomechanical system made of one electromagnetic field that is driving two mechanically coupled mechanical resonators. The phonon hopping rate between the two resonators is modulated in order to induce a synthetic magnetism. Moreover, one of the resonator supports a Duffing nonlinearity. By using experimentally feasible parameters, we have shown that the stability of the system is slightly improved, which is a good requirement to enhance stationary entanglement. When the system is free of the Duffing nonlinearity, we have shown that the logarithmic negativity features a phenomenon of sudden death and revival of entanglement. The optimal values of the entanglement appear around the synthetic phase of $\theta = m\frac{\pi}{2}$, and they switch out as this phase meets $\theta = n\pi$, where m is an odd number and n is an integer. After appropriately setting the synthetic phase, we observed that the entanglement be-

tween the electromagnetic field and the resonator supporting the Duffing nonlinearity becomes weak and tends to switch out for strong enough nonlinearity. However, the entanglement is switched towards the resonator that is free of the Duffing term, leading to a sort of nonlinear-assisted transfer of entanglement. This transferred entanglement has been shown to be robust enough against thermal fluctuation. Our work paves a way towards nonlinear transfer entanglement phenomenon in complex system. These results can be used to generate robust and stable entanglement in nonlinear system, which is interesting for quantum information processing and quantum computing purposes.

Acknowledgments

This work has been carried out under the Iso-Lomso Fellowship at Stellenbosch Institute for Advanced Study

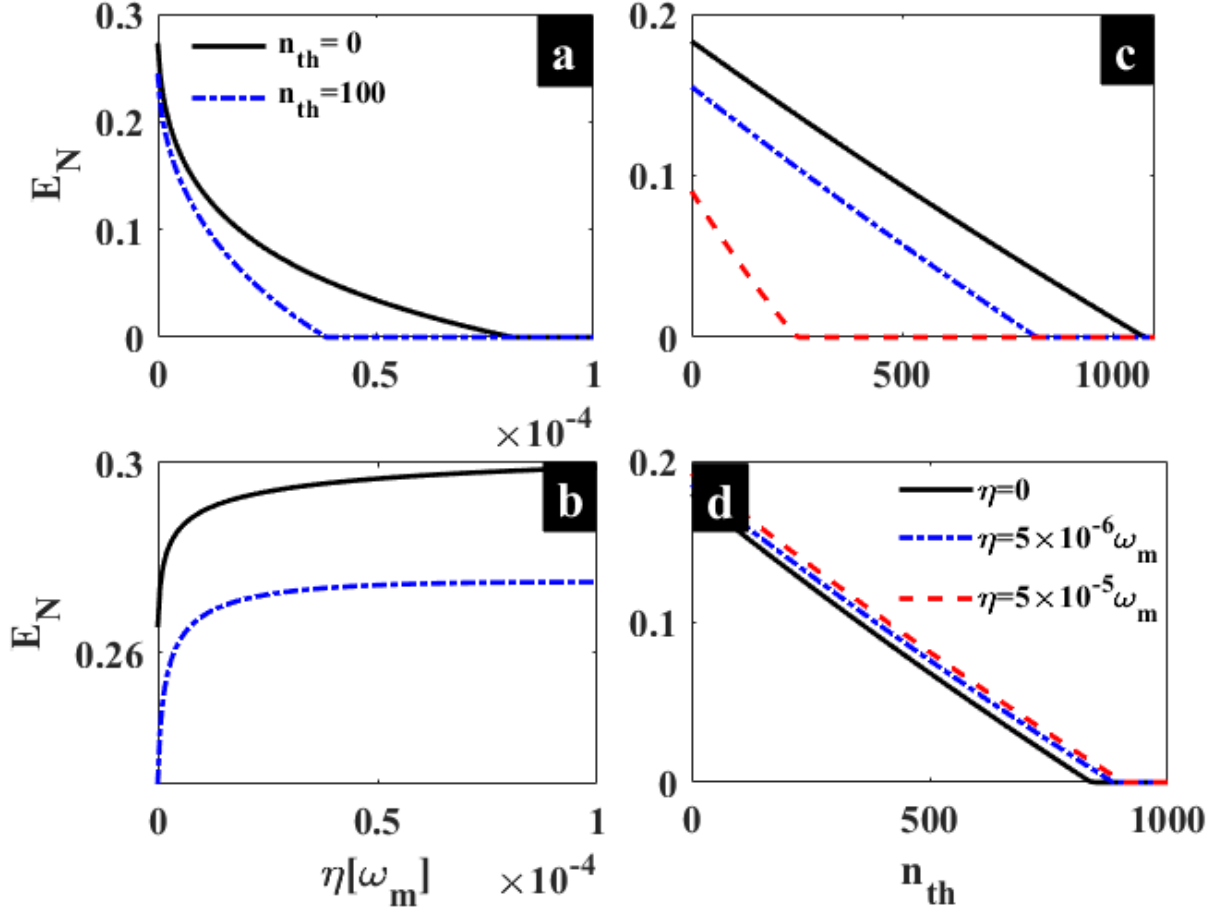


FIG. 5: Entanglement between the electromagnetic field with the nonlinear resonator (a), and with the linear resonator (b) versus the nonlinear term η . Entanglement between the electromagnetic field with the nonlinear resonator (c), and with the linear resonator (d) versus the thermal phonon number n_{th} . In (a,b), the solid line is for $n_{th}=0$ and the dashed line is for $n_{th}=100$. In (c,d), the solid line is without Duffing nonlinearity ($\eta = 0$), while the dash-dotted and dashed lines are for $\eta = 5 \times 10^{-6} \omega_m$ and $\eta = 5 \times 10^{-5} \omega_m$, respectively. The driving field is $\alpha^{in} = 1500$ in (a,b) and $\alpha^{in} = 1000$ in (c,d). The rest of the parameters are as in Fig.3.

(STIAS), Wallenberg Research Centre at Stellenbosch University, Stellenbosch 7600, South Africa. P. Djorwe acknowl-

edges the receipt of a grant from the APS-EPS-FECS-ICTP Travel Award Fellowship Programme (ATAP), Trieste, Italy.

-
- [1] A. Pokharel, H. Xu, S. Venkatachalam, E. Collin, and X. Zhou, Nano Letters **22**, 7351 (2022), ISSN 1530-6992.
- [2] I. Golokolenov, D. Cattiaux, S. Kumar, M. Sillanpää, L. Mercier de Lépinay, A. Fefferman, and E. Collin, New Journal of Physics **23**, 053008 (2021), ISSN 1367-2630.
- [3] D. P. Foulla, P. Djorwé, S. T. Kingni, and S. G. N. Engo, Physical Review A **95** (2017).
- [4] S. Walter and F. Marquardt, New Journal of Physics **18**, 113029 (2016), ISSN 1367-2630.
- [5] P. Djorwé, J. H. Talla Mbé, S. G. Nana Engo, and P. Wofo, The European Physical Journal D **67**, 1 (2013), URL <https://doi.org/10.1140/epjd/e2013-30581-0>.
- [6] M.-A. Lemonde, N. Didier, and A. A. Clerk, Nature Communications **7** (2016), ISSN 2041-1723, URL <https://doi.org/10.1038/ncomms11338>.
- [7] S. Barzanjeh, A. Xuereb, S. Gröblacher, M. Paternostro, C. A. Regal, and E. M. Weig, Nature Physics **18**, 15 (2021), ISSN 1745-2481.
- [8] M. Aspelmeyer, S. Gröblacher, K. Hammerer, and N. Kiesel, Journal of the Optical Society of America B **27**, A189 (2010), ISSN 1520-8540.
- [9] P. Djorwé, J. H. T. Mbé, S. G. N. Engo, and P. Wofo, Physical Review A **86** (2012).
- [10] M. Colombano, G. Arregui, N. Capuj, A. Pitanti, J. Maire, A. Griol, B. Garrido, A. Martinez, C. Sotomayor-Torres, and D. Navarro-Urrios, Physical Review Letters **123**, 017402 (2019), ISSN 1079-7114.
- [11] C. C. Rodrigues, C. M. Kersul, A. G. Primo, M. Lipson, T. P. M.

- Alegre, and G. S. Wiederhecker, *Nature Communications* **12** (2021), ISSN 2041-1723.
- [12] P. Djourwé, Y. Pennec, and B. Djafari-Rouhani, *Physical Review B* **102**, 155410 (2020).
- [13] J. Li, Z.-H. Zhou, S. Wan, Y.-L. Zhang, Z. Shen, M. Li, C.-L. Zou, G.-C. Guo, and C.-H. Dong, *Physical Review Letters* **129**, 063605 (2022), ISSN 1079-7114.
- [14] P. Djourwe, Y. Pennec, and B. Djafari-Rouhani, *Scientific Reports* **9**, 1684 (2019), URL <https://api.semanticscholar.org/CorpusID:59617258>.
- [15] D. Navarro-Urrios, N. E. Capuj, M. F. Colombano, P. D. García, M. Sledzinska, F. Alzina, A. Griol, A. Martínez, and C. M. Sotomayor-Torres, *Nature Communications* **8** (2017), ISSN 2041-1723.
- [16] T. F. Roque, F. Marquardt, and O. M. Yevtushenko, *New Journal of Physics* **22**, 013049 (2020), ISSN 1367-2630.
- [17] P. Djourwe, J. Yves Effa, and S. G. Nana Engo, *Nonlinear Dynamics* **111**, 5905 (2022), ISSN 1573-269X.
- [18] G.-L. Zhu, C.-S. Hu, Y. Wu, and X.-Y. Lü, *Fundamental Research* **3**, 63 (2023), ISSN 2667-3258.
- [19] M. T. Stella, P. Djourwe, T. Murielle, and N. E. Serge Guy, *Physica Scripta* (2023), ISSN 1402-4896.
- [20] T. P. Purdy, K. E. Grutter, K. Srinivasan, and J. M. Taylor, *Science* **356**, 1265 (2017), ISSN 1095-9203.
- [21] F. Bemani, R. Roknizadeh, A. Motazedifard, M. H. Naderi, and D. Vitali, *Physical Review A* **99**, 063814 (2019), ISSN 2469-9934.
- [22] R. Riedinger, S. Hong, R. A. Norte, J. A. Slater, J. Shang, A. G. Krause, V. Anant, M. Aspelmeyer, and S. Gröblacher, *Nature* **530**, 313 (2016), ISSN 1476-4687.
- [23] A. Zivari, R. Stockill, N. Fiaschi, and S. Gröblacher, *Nature Physics* **18**, 789 (2022), ISSN 1745-2481.
- [24] N. Fiaschi, B. Hensen, A. Wallucks, R. Benevides, J. Li, T. P. M. Alegre, and S. Gröblacher, *Nature Photonics* **15**, 817 (2021), ISSN 1749-4893.
- [25] P. Djourwé, S. N. Engo, J. T. Mbé, and P. Wofo, *Physica B: Condensed Matter* **422**, 72 (2013).
- [26] P. Banerjee, S. Kalita, and A. K. Sarma, *Journal of the Optical Society of America B* **40**, 1398 (2023), ISSN 1520-8540.
- [27] R. Riedinger, A. Wallucks, I. Marinković, C. Löschnauer, M. Aspelmeyer, S. Hong, and S. Gröblacher, *Nature* **556**, 473 (2018), ISSN 1476-4687.
- [28] S. Kotler, G. A. Peterson, E. Shojaee, F. Lecocq, K. Cicak, A. Kwiatkowski, S. Geller, S. Glancy, E. Knill, R. W. Simmonds, et al., *Science* **372**, 622 (2021), ISSN 1095-9203.
- [29] L. Mercier de Lépinay, C. F. Ockeloen-Korppi, M. J. Woolley, and M. A. Sillanpää, *Science* **372**, 625 (2021), ISSN 1095-9203.
- [30] N. Meher and S. Sivakumar, *The European Physical Journal Plus* **137** (2022), ISSN 2190-5444.
- [31] S. Slussarenko and G. J. Pryde, *Applied Physics Reviews* **6** (2019), ISSN 1931-9401.
- [32] F. Arute, K. Arya, R. Babbush, D. Bacon, J. C. Bardin, R. Barends, R. Biswas, S. Boixo, F. G. S. L. Brandao, D. A. Buell, et al., *Nature* **574**, 505 (2019), ISSN 1476-4687.
- [33] Y. Xia, A. R. Agrawal, C. M. Pluchar, A. J. Brady, Z. Liu, Q. Zhuang, D. J. Wilson, and Z. Zhang, *Nature Photonics* **17**, 470 (2023), ISSN 1749-4893.
- [34] S. Chakraborty and A. K. Sarma, *Physical Review A* **100**, 063846 (2019), ISSN 2469-9934.
- [35] D.-G. Lai, J.-Q. Liao, A. Miranowicz, and F. Nori, *Physical Review Letters* **129**, 063602 (2022).
- [36] S. Venkatachalam and X. Zhou, *Nanotechnology* **34**, 215202 (2023), ISSN 1361-6528.